AIP Conference Proceedings

Microcapsules of poly(methyl metharcylate) containing epoxy resin and multi-walled carbon nanotubes

Cite as: AIP Conference Proceedings **1914**, 030017 (2017); https://doi.org/10.1063/1.5016704
Published Online: 15 December 2017

M. Galip Icduygu, Meltem Asilturk, and M. Cengiz Altan

View Online Export Citation

ARTICLES YOU MAY BE INTERESTED IN

Preparation and characterisation of user-friendly PMMA microcapsules for consumer care
AIP Conference Proceedings **1542**, 1027 (2013); https://doi.org/10.1063/1.4812109

Autonomic restoration of electrical conductivity using polymer-stabilized carbon nanotube and graphene microcapsules
Applied Physics Letters **101**, 043106 (2012); https://doi.org/10.1063/1.4737935

Lap shear strength and healing capability of self-healing adhesive containing epoxy/ mercaptan microcapsules
AIP Conference Proceedings **1713**, 140004 (2016); https://doi.org/10.1063/1.4942339

Challenge us.
What are your needs for periodic signal detection?
Watch

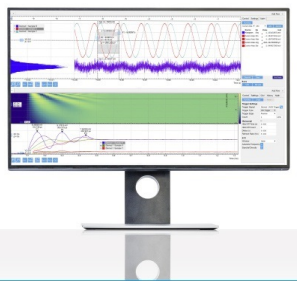

Zurich Instruments

AIP Publishing

© 2017 Author(s).

Microcapsules of Poly(methyl metharcylate) Containing Epoxy Resin and Multi-Walled Carbon Nanotubes

M. Galip Icduygu[a,1] Meltem Asilturk[b] and M. Cengiz Altan[c, 2]

[a] *School of Civil Aviation, Giresun University, Giresun TURKEY*
[b] *Material Science and Engineering Department, Akdeniz University, Antalya, TURKEY*
[c] *School of Aerospace and Mechanical Engineering, University of Oklahoma, Norman, OK, USA*

[1] *mehmet.icduygu@giresun.edu.tr*
[2] *altan@ou.edu*

Microcapsules of poly(methyl methacrylate) [PMMA] containing epoxy and multi-walled carbon nanotubes were formed by solution evaporation in an aqueous emulsion. Thin PMMA shells precipitated at the resin/water interface as the solvent was removed, thus encapsulating the dispersion of epoxy and nanotubes. Dichloromethane (DCM) was selected as the common solvent for both resin and PMMA, and slowly evaporated from the aqueous mixture agitated at 40ºC. After trying various epoxy/PMMA ratios, a 1:1 w/w epoxy/PMMA ratio yielded stable, individual microcapsules with smooth PMMA shells. Four different mixing speeds (300, 500, 800, and 1000 rpm) and four carbon nanotube contents (0.25, 0.50, 1.00, 2.00 w/w %) were used during the encapsulation process. Microcapsules with 10 to 55 μm average diameter were obtained by increasing the mixing speed from 300 to 1000 rpm. Increasing the mixing speed yielded a decrease in average particle size, whereas carbon nanotube presence led to a broader capsule size distribution at any given mixing speed. In addition, roughness of the microcapsule surface increased with increasing carbon nanotube content and mixing speed. SEM images of microcapsules showed that microcapsules with various types of core-shell morphology were formed during the encapsulation process.

Keywords: Self-healing composites, PMMA microcapsules, carbon nanotube, epoxy
PACS: 81

INTRODUCTION

Micro encapsulation is a well-known technique in which solids, liquids, or gases can be enclosed in a thin-shelled, spherical capsule having a diameter between a few micrometers to millimeters. These microcapsules have been used in various industrial applications such as pharmaceuticals, adhesives, and cosmetics. More recently, microcapsules containing thermosetting resins have been successfully used in fabricating self-healing composites. Typically, externally induced damage in a composite is "healed" by mixing and curing the resin and hardener, released from the fractured microcapsules embedded in the composite. Formation of microcapsules by a wide variety of polymers and nanomaterials as shell and/or core materials have been reported in recent studies [1-5]. In two-component self-healing systems, such as thermoset (resin/hardener) or thermoplastic (monomer/initiator) systems, both components may be placed in the same capsules or in separate capsules of appropriate sizes. Nanomaterials such as carbon nanotubes have also been incorporated into microcapsules as an additional component. For example, Caruso et al. [6] synthesized microcapsules containing carbon nanotubes (CNTs) using an *in situ* emulsification polymerization of urea–formaldehyde for damage sensing. In addition, autonomic restoration of electrical conductivity using polymer-stabilized carbon nanotubes and graphene microcapsules has been studied by Odom et al. [7].

Solvent evaporation has been extensively used in encapsulation of self-healing materials. Epoxy and diamines are two example materials that can be encapsulated by using the solvent evaporation approach. In this approach, self-healing materials and a shell-forming polymer are dissolved in an organic solvent and dispersed in an aqueous phase. A hard shell is formed, encapsulating epoxy or hardener micro droplets after evaporation of the solvent. When used with epoxy and dissolved in dichloromethane (DCM), poly(methyl methacrylate) (PMMA) forms smooth shells around the epoxy droplets after DCM is removed from the solution [8-9].

The encapsulation of epoxy/carbon nanotube dispersions by PMMA through solvent evaporation technique has not been reported in the literature. The purpose of this study is to investigate the possible use of solvent evaporation technique to prepare microcapsules containing epoxy/carbon nanotube dispersion with PMMA shells that are suitable for self-healing composites.

Proceedings of PPS-32
AIP Conf. Proc. 1914, 030017-1–030017-5; https://doi.org/10.1063/1.5016704
Published by AIP Publishing. 978-0-7354-1606-2/$30.00

MATERIALS AND METHODS

EPON 828 was used as the low-viscosity epoxy resin (Miller Stephenson Chemical Co.). Dichloromethane (DCM), poly(methyl methacrylate) [Mw~120000], sodium dodecyl sulfate (SDS) and multi-walled carbon nanotube (MWNT) [>90% carbon, D × L: 110-170 nm × 5-9 μm] (Sigma Aldrich) were used without any further processing or purification.

Preparation of Microcapsules

Four different mixing speeds (300, 500, 800 and 1000 rpm) and four multi-walled carbon nanotube (MWNT) contents (0.25, 0.50, 1.00, and 2.00 % wt. fiber/resin) were used to prepare the microcapsules. MWNT, EPON 828 and PMMA weighed in appropriate ratios and mixed in 60 ml DCM on a magnetic stirrer until EPON 828 and PMMA completely dissolved in DCM. This mixture was sonicated by using a Vibra-Cell high intensity ultrasonic processor for 10 minutes to enhance MWNT dispersion. Forty ml of this mixture was added to a 50-ml 1% w/V aqueous SDS solution drop-by-drop over a 90-minute period to get the organic phase/water emulsion at the desired mixing rate. After the emulsion was stabilized, the mixture was added to a 200-ml 1% w/V SDS solution and the temperature of the mixture was raised to 40ºC. After 4 hours, the mixture was cooled to room temperature and filtered by using Whatman Grade 93 filter paper. Filtered microcapsules were washed with excess distilled water and dried at room temperature under the fume hood.

Characterization of Microcapsules

Chemical analyses of microcapsules were carried out by a Bruker IFS 66/S Fourier Transform Infrared Instrument. A Zeiss NEON 40 EsB Scanning Electron Microscope (SEM) was used to characterize both the surface and shell morphology of the microcapsules. Test samples were prepared on a glass slide and coated by using Hummer VI Triode Sputter Coater.

RESULTS AND DISCUSSION

FTIR Characterization

Figure 1 shows the Fourier Transform Infrared (FTIR) spectrum of the microcapsules prepared with different nanotube contents and mixing rates.

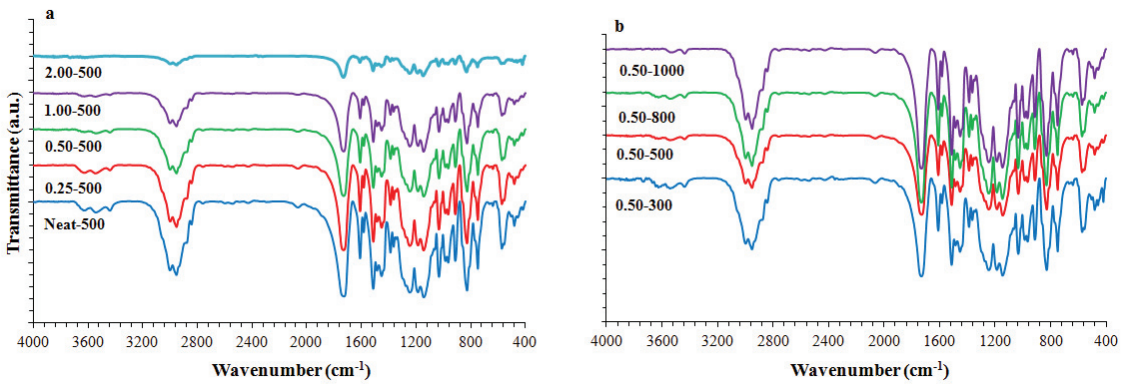

FIGURE 1. The FTIR spectrum of microcapsule prepared at (a) various nanotube/resin weight ratios at 500 rpm and (b) various mixing rates at 0.50 % wt. of MWNT/EPON 828.

The FTIR spectra of the microcapsules show characteristic PMMA absorption bands between 1,150 and 1,250 cm^{-1}, which can be attributed to the C-O-C stretching vibrations. The bands at 1,388 cm^{-1} and 754 cm^{-1} correspond to the α-methyl group vibrations. EPON 828 shows absorbing bands in the O-H stretching region (3200-3650 cm^{-1}), and the aliphatic C-H stretching bands are observed at 2860-3060 cm^{-1}. The C=C phenyl ring stretching bands appear at 1620 and 1462 cm^{-1} and the symmetric stretching band of epoxy ring can be seen at 1250 cm^{-1}. Hence, presence of EPON 828 and PMMA is evident in all microcapsule samples.

Particle Size Distribution

Particle size distribution of the microcapsules was determined by analyzing of SEM images. Multiple images taken at 50X magnification were utilized to determine the particle size distribution for each sample. Table 1 shows the mean and standard deviation values of the microcapsule diameter. As shown in Table 1, the presence of MWNT did not have a significant effect on the capsule size distribution for microcapsules prepared at 500 rpm. These microcapsules had average capsule diameters ranging between 27 and 31 μm for most cases. The mean particle size was slightly reduced when nanotube content increased to 2 % wt. The most apparent difference in the capsule size resulted from changing the mixing speed. Both the mean and the standard deviation of capsule diameter considerably decreased with increasing mixing speed.

TABLE 1. Particle size distribution of microcapsules.

Sample Codes MWNT (% wt.)-rpm	Mean Capsule Diameter (μm)	Standard Deviation (μm)
Neat-500	29.37	11.09
0.25-500	27.32	10.06
0.50-500	31.34	19.47
1.00-500	29.06	13.77
2.00-500	23.11	11.87
0.5-300	55.23	22.17
0.5-500	31.34	19.47
0.5-800	17.65	11.95
0.5-1000	10.34	9.30
Neat-1000	12.99	6.90

Microcapsule Morphology

The SEM images, depicted in Fig. 2, revealed that the microcapsules with multi-walled carbon nanotubes had a rougher surface morphology than the neat capsules. As shown in Figs. 2b and 2d, roughness was mainly caused by the presence of nanotubes, which were clearly visible at the capsule surface even at the low nanotube weight fraction of 0.5 %, covered by a thin layer of PMMA. Nanotubes appeared either as isolated, individual tubes, or as clusters. These clusters were formed by several entangled and nearly collimated nanotubes. Many of the nanotubes seemed to conform to the surface curvature of the capsule and were somewhat aligned near each other, forming a discernable but local preferred orientation. In other words, the location and alignment of the nanotubes on the surface appeared to be affected by the presence of other nanotubes within their proximity, even though they were not necessarily in physical contact or part of a larger cluster. Occasionally, nanotubes were not straight and bend with a very small radius of curvature. It is highly unlikely that these nanotubes were bent during the formation of the microcapsule, since one does not expect sufficiently high compressive stresses in the tangential direction to buckle the nanotube on the capsule surface. On the other hand, it is possible that these tubes were bent when they were initially synthesized, and retained their shape during encapsulation. It is worth noting that the nanotube clusters do not exhibit a spatially uniform and observable preferred alignment direction on the capsule surface.

Another prominent morphological feature of the surface of these capsules was several impact craters of various sizes. These craters may have been formed by the collision of microcapsules as they were being agitated at high speeds in the aqueous suspension. These collisions could have been highly plastic in nature, and thus, might have led to the formation of larger aggregates of multiple capsules adhering to each other after the collision, especially if the capsule surfaces were sufficiently soft. The mixing speed and capsule size distribution were likely to affect the formation of these aggregates as well as the adhesion of the capsules after collision. The microcapsule aggregates could be separated either after the shells were hardened or during the washing/drying steps, thus yielding a surface morphology observed in Fig. 2. This effect was especially visible at the 1000 rpm mixing rate due to the increase in both the number and strength of the collisions between the microcapsules during the encapsulation process.

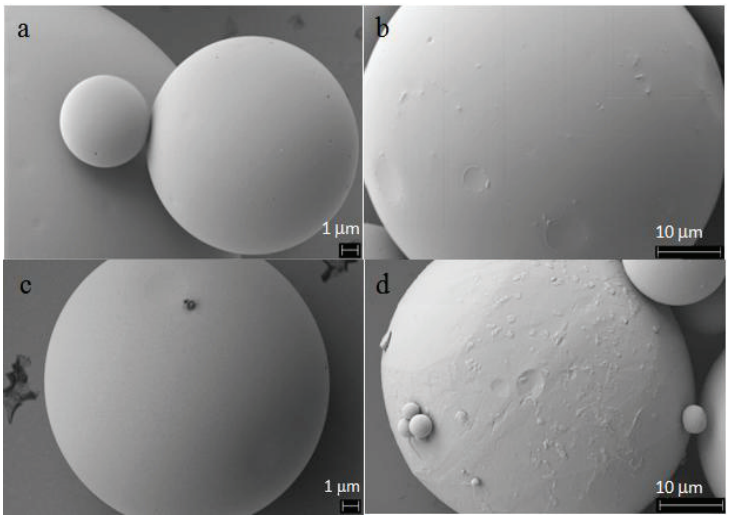

FIGURE 2. Surface morphology of microcapsules with and without MWNT:
(a) Neat PMMA at 500 rpm, (b) 0.5 % MWNT at 500 rpm, (c) Neat PMMA at 1000 rpm, and (d) 0.5 % MWNT at 1000 rpm.

When mixing speed was kept constant and the MWNT content was increased, the surface of the microcapsules started to contain more nanotubes as shown in Fig. 3. The size of the nanotube clusters increased, and they became more isotropic (Fig. 3c) as untangling and aligning a larger number of nanotubes on the capsule surface became more difficult. Increasing the nanotube content in the PMMA shell would enhance the shell strength and stiffness, but also decrease the flexibility of the capsules. Hence, at higher nanotube loadings, brittle fractures were observed on the capsules as shown in Fig. 3d. Collisions between stiffer capsules seemed to induce these eggshell-type fractures instead of leaving an impact crater on the surface as observed for capsules at lower nanotube content.

Some level of variation in shell morphology was observed even within capsules from the same sample as shown in Fig. 4. A particular sample set may exhibit a non-uniform shell thickness. In fact, in many cases, multiple sub-micron pin holes were observed on the interior surface of the PMMA as shown in Fig. 4a. Spherical particles with a homogenous, solid core were also formed during the encapsulation process (Fig. 4d). The interior shell structure showed variations from sample to sample and was either solid or contained entrapped voids across the shell wall. The presence of carbon nanotubes embedded through the shell thickness can also be seen in Fig. 4a.

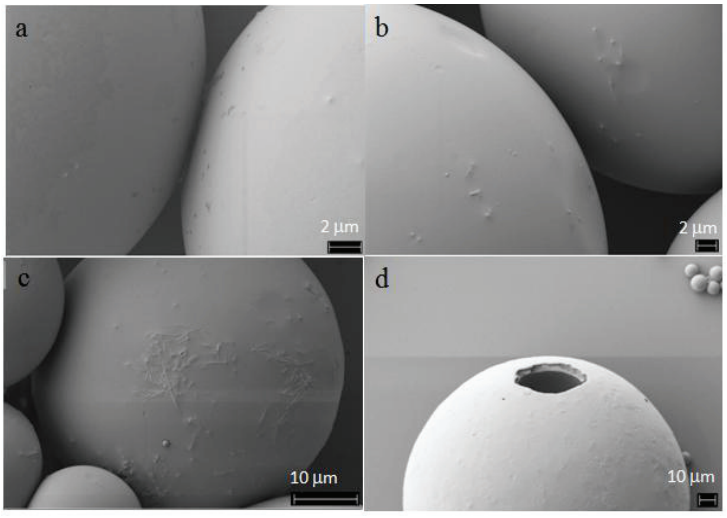

FIGURE 3. Surface morphology of microcapsules formed at 500 rpm mixing speed showing the effect of increased MWNT content: (a) 0.25 % wt., (b) 0.5 % wt., (c) 1.0 % wt., and (d) 2.0 % wt.

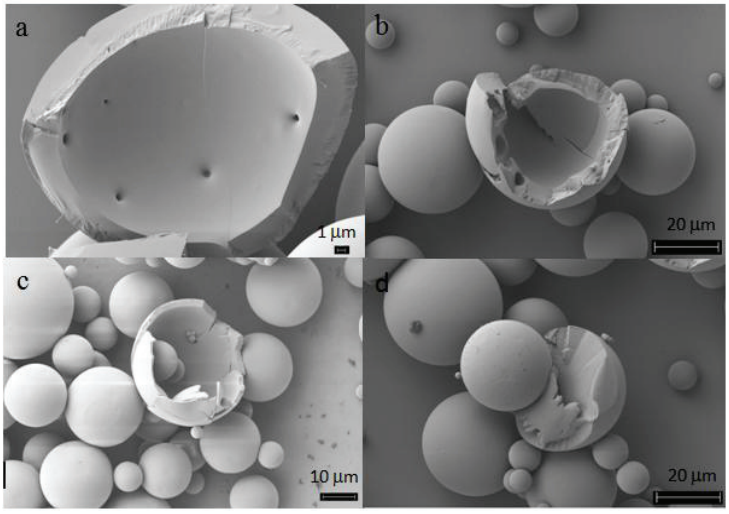

FIGURE 4. Shell and interior morphology of microcapsules: (a) 0.50 % wt. MWNT at 500 rpm, (b) Neat microcapsules at 500 rpm, (c) Neat microcapsule at 1000 rpm, and (d) Neat microcapsules at 500 rpm.

CONCLUSION

Microcapsules containing epoxy/carbon nanotube dispersion were successfully synthesized by using PMMA as a shell material. Multi-walled carbon nanotube content up to 2 % wt. was dispersed in an epoxy resin/PMMA solution dissolved in dichloromethane (DCM). Epoxy/carbon nanotube dispersion was subsequently encapsulated by PMMA via the evaporation of the solvent in an aqueous solution. It was possible to reduce the average diameter of microcapsules from 55 to 13 µm by increasing the mixing speed from 300 to 1000 rpm. Microcapsules exhibited sub-micron surface roughness due to the presence of nanotubes covered by a thin layer of PMMA at the surface. At the surface, both a number of single, isolated nanotubes and clusters comprised of several nanotubes were observed. In addition, impact craters of various sizes were often seen on the capsule surface due to collisions among microcapsules that were facilitated by agitation of the aqueous suspension. Increasing the carbon nanotube content created a more rigid shell that exhibited brittle fracture. The ability to tailor the shell stiffness and strength by changing the MWNT content could be especially beneficial in self-healing applications of composite laminates.

ACKNOWLEDGMENTS

The authors would like to thank Dr. Preston Larson from the Samuel Noble Microscopy Laboratory at the University of Oklahoma for SEM imaging of the microcapsules.

REFERENCES

1. H. Jin, C. L. Mangun, D. S. Stradley, S.M. Moore, N. R. Sottos, S. R. White, *Polymer* **53**, 581-587 (2012).
2. B. J. Blaiszik, M. M. Caruso, D. A. McIlroy, J.S. Moore, S. R. White, N. R. Sottos, *Polymer* **50**, 990-997 (2009).
3. C. Y. Zhang, X. B. Jiang, M. Z. Rong, M.Q. Zhang, *Journal Of Intelligent Material Systems and Structures* **25**, 31-39 (2014).
4. H. Wang, Y. Yuan, M. Rong, M. Zhang, *Colloid and Polymer Science* **287**, 1089-1097 (2009).
5. G. O. Wilson, J. W. Henderson, M. M. Caruso, B. J. Blaiszik, P.J. McIntire, N. R. Sottos, S. R. White, J. S. Moore, *Journal of Polymer Science Part A-Polymer Chemistry* **48**, 2698-2708 (2010).
6. M. M. Caruso, S. R. Schelkopf, A. C. Jackson, A. M. Landry, P.V. Braun, J. S. Moore, *Journal of Material Chemistry* **19**, 6093-6096 (2009).
7. S. A. Odom, T. P. Tyler, M. M. Caruso, J.A. Ritchey, M.V. Schulmerich, S. J. Robinson, R. Bhargava, N. R. Sottos, S. R. White, M. C. Hersam, J. S. Moore, *Applied Physics Letters* **101**, 043106 (2012) .
8. Q. Li, K. Siddaramaiah, H. K. Nam, D. Hui, J. H. Lee, *Composites Part B- Engineering* **55**, 79-85 (2013).
9. Q. Li, A. K. Mishra, N. H. Kim, T. Kuila, K. Lau, J. H. Lee, *Composites Part B-Engineering* **49**, 6-15 (2013).